

**Electronic Supplementary Material (ESI) for New Journal of Chemistry**

Electronic Supporting Information

**A cellulose substance derived nanofibrous CoS-nanoparticle/carbon composite as a high-performance anodic material for Lithium-ion batteries**

Hang Yuan,<sup>a</sup> Fan Wang,<sup>a</sup> Shun Li,<sup>b</sup> Zehao Lin<sup>a</sup> and Jianguo Huang<sup>\*,a</sup>

<sup>a</sup> Department of Chemistry, Zhejiang University, Hangzhou, Zhejiang 310027, China

<sup>b</sup> School of Engineering, Zhejiang A&F University, Hangzhou, Zhejiang 311300, China

E-mail: jghuang@zju.edu.cn

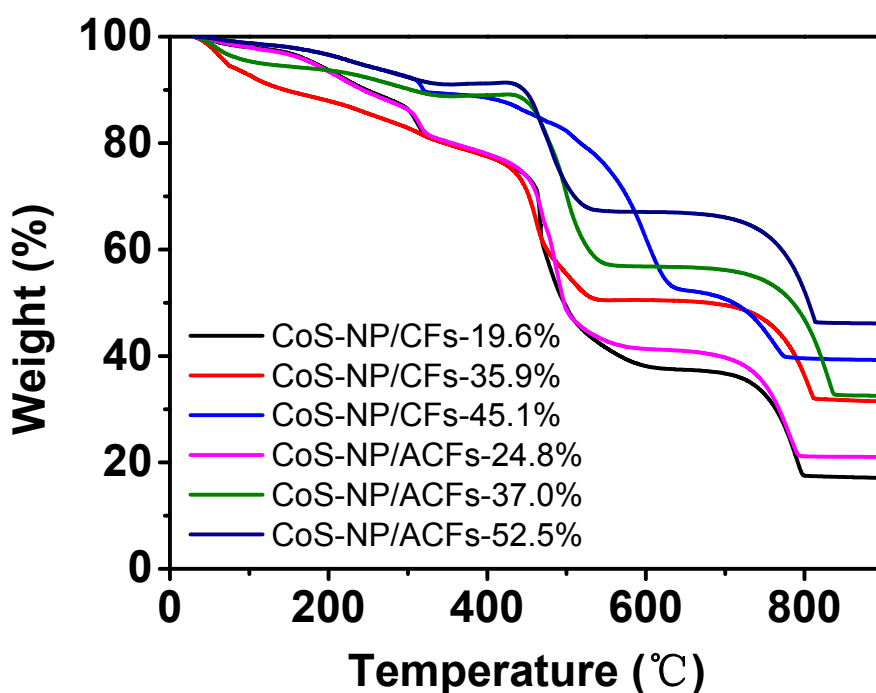


**Fig. S1** Thermogravimetric curves of the CoS-NP/CFs-19.6%, CoS-NP/CFs-35.9%, CoS-NP/CFs-45.1%, CoS-NP/ACFs-24.8%, CoS-NP/ACFs-37.0% and CoS-NP/ACFs-52.5% composites.

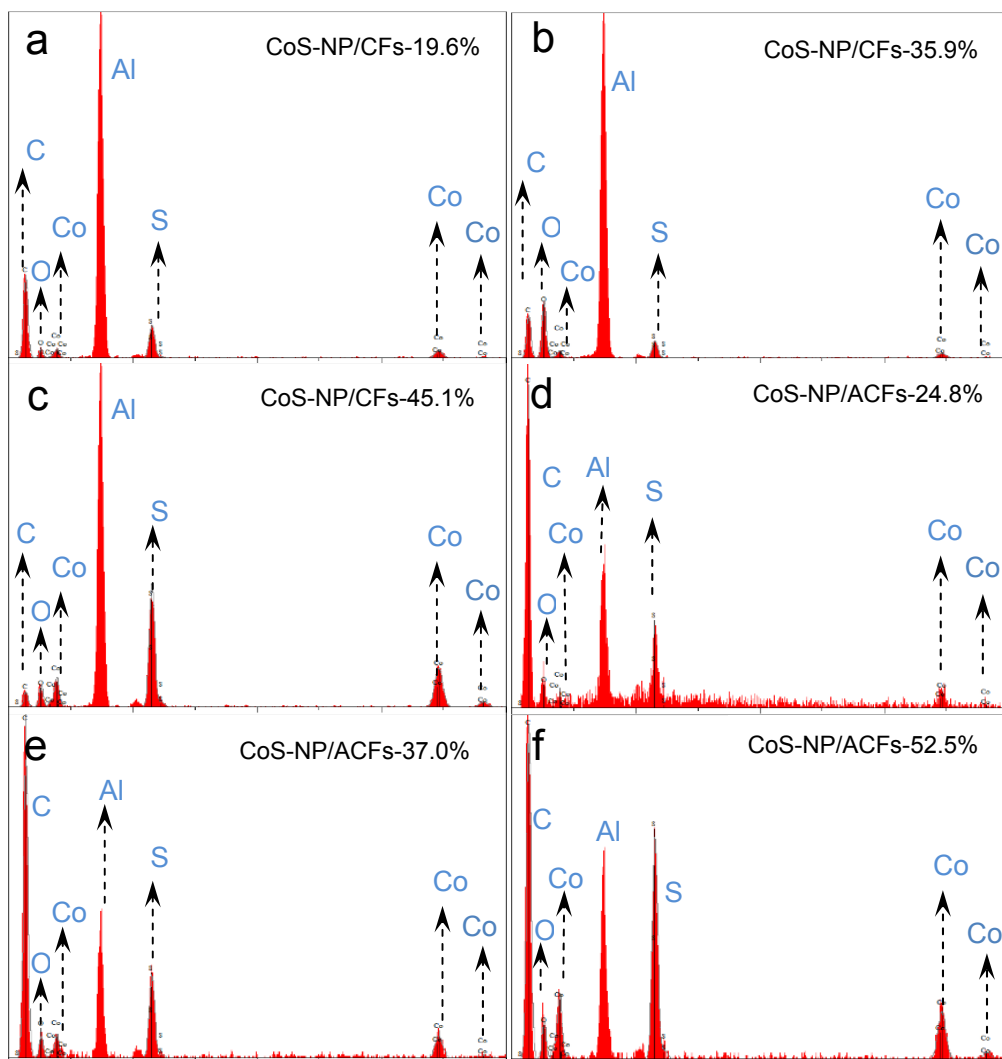


**Fig. S2** EDX analyses of the a) CoS-NP/CFs-19.6%, b) CoS-NP/CFs-35.9%, c) CoS-NP/CFs-45.1%, d) CoS-NP/ACFs-24.8%, e) CoS-NP/ACFs-37.0% and f) CoS-NP/ACFs-52.5% composites. The Al signal came from the aluminum foil substrate that was used to support the specimens. The CoS contents revealed by the EDX data of the CoS-NP/CFs series samples are correspondingly 18.0%, 34.0% and 43.2% by weight; and those for the CoS-NP/ACFs series samples are correspondingly 22.3%, 36.2% and 65.9% by weight.

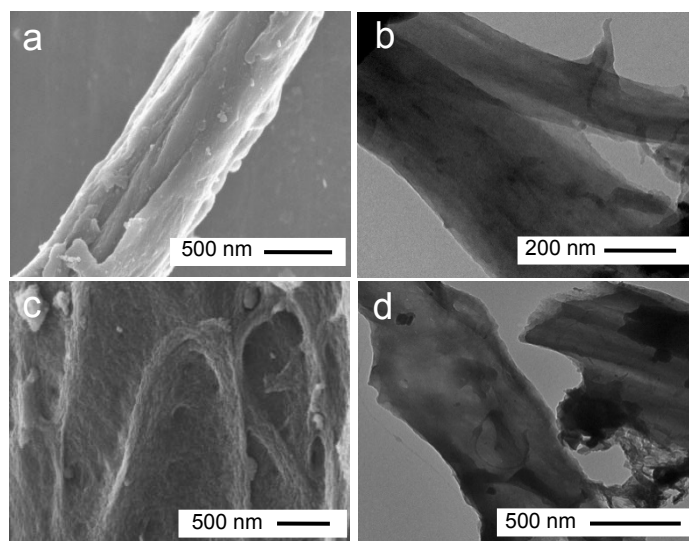


**Fig. S3** Electron micrographs of the carbon fibres derived from filter paper. a, b) FE-SEM and TEM images of the carbon fibres obtained by carbonization of the filter paper at 450 °C, showing the smooth surface of it; c, d) FE-SEM and TEM images of carbon fibres activated by KOH in an argon atmosphere at 800 °C for 2.5 hours, showing the rougher surface and porous structure.

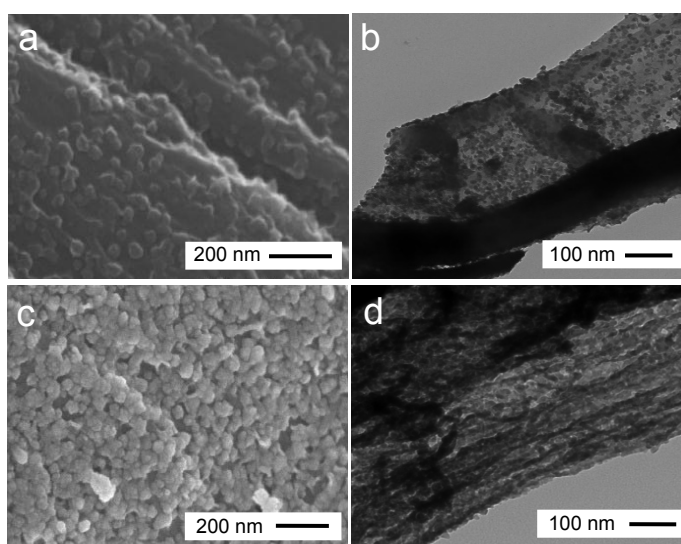


**Fig. S4** Electron micrographs of the CoS-NP/ACFs-24.8% and CoS-NP/ACFs-52.5% composites. a, b) FE-SEM and TEM images of the CoS-NP/ACFs-24.8% composite, showing the sparse distribution of CoS nanoparticles; c, d) FE-SEM images of the CoS-NP/ACFs-52.5% composite, showing the high loading density of CoS nanoparticle on the surface of activated

carbon fibre.

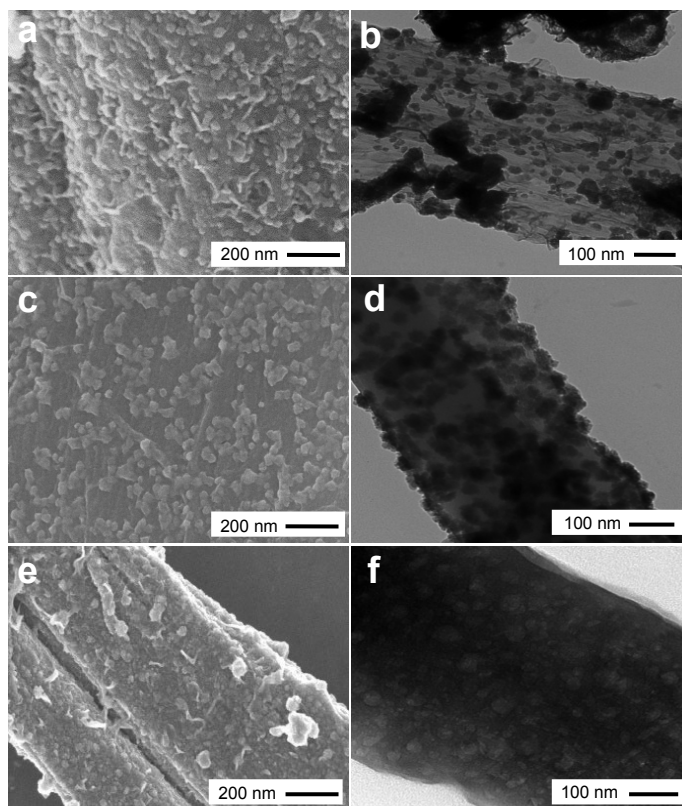


**Fig. S5** SEM and TEM micrographs of the CoS-NP/CFs-19.6% composite (a,b), the CoS-NP/CFs-35.9% composite (c,d) and the CoS-NP/CFs-45.1% composite (e,f).

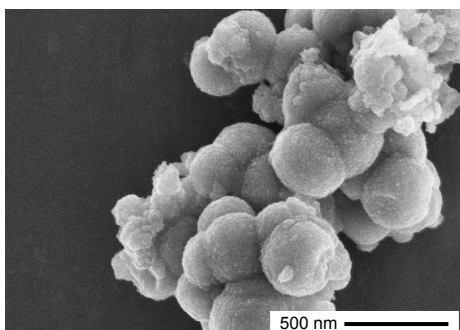


**Fig. S6** FE-SEM micrographs of the CoS powder sample, showing aggregated spherical particles with a diameter of about 300 nm.

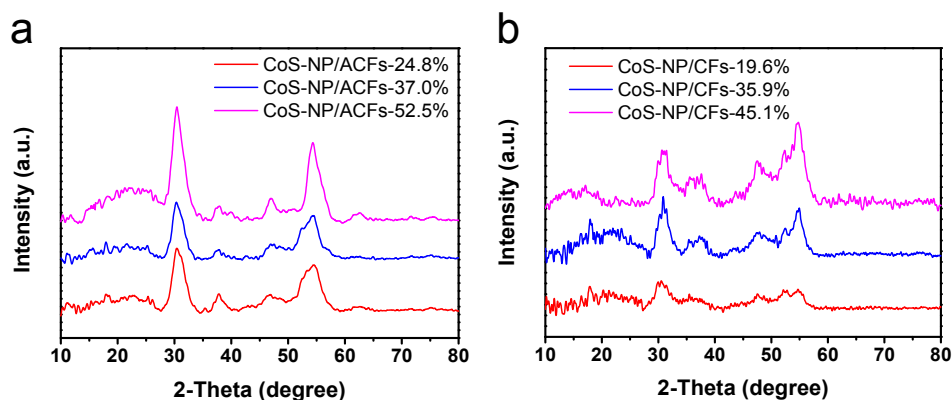


**Fig. S7** X-ray diffraction patterns of the CoS-NP/ACFs-24.8%, CoS-NP/ACFs-37.0%, CoS-NP/ACFs-52.5% samples (a) and the CoS-NP/CFs-19.6%, CoS-NP/CFs-35.9%, CoS-NP/CFs-45.1% samples (b).

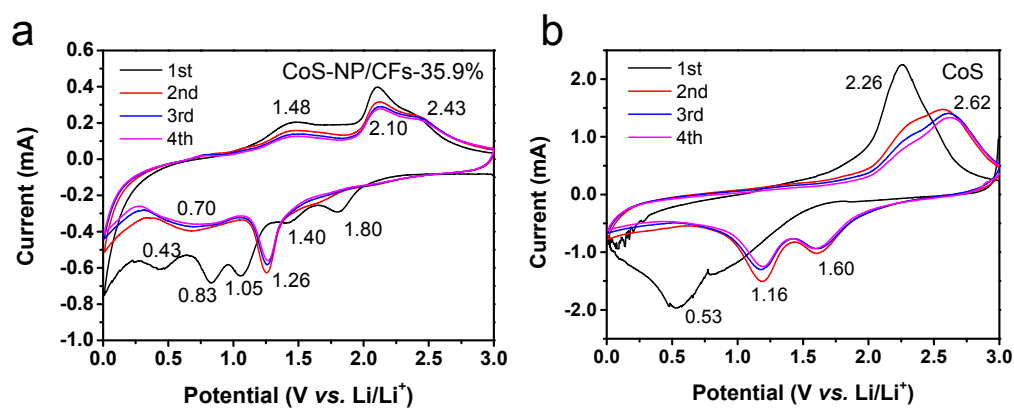


**Fig. S8** The CV curves of a) the CoS-NP/CFs-35.9% based anode and b) the CoS powder based anode at a scan rate of  $0.5 \text{ mV s}^{-1}$  over the voltage range of 0.01–3.0 V vs. Li/Li<sup>+</sup>.

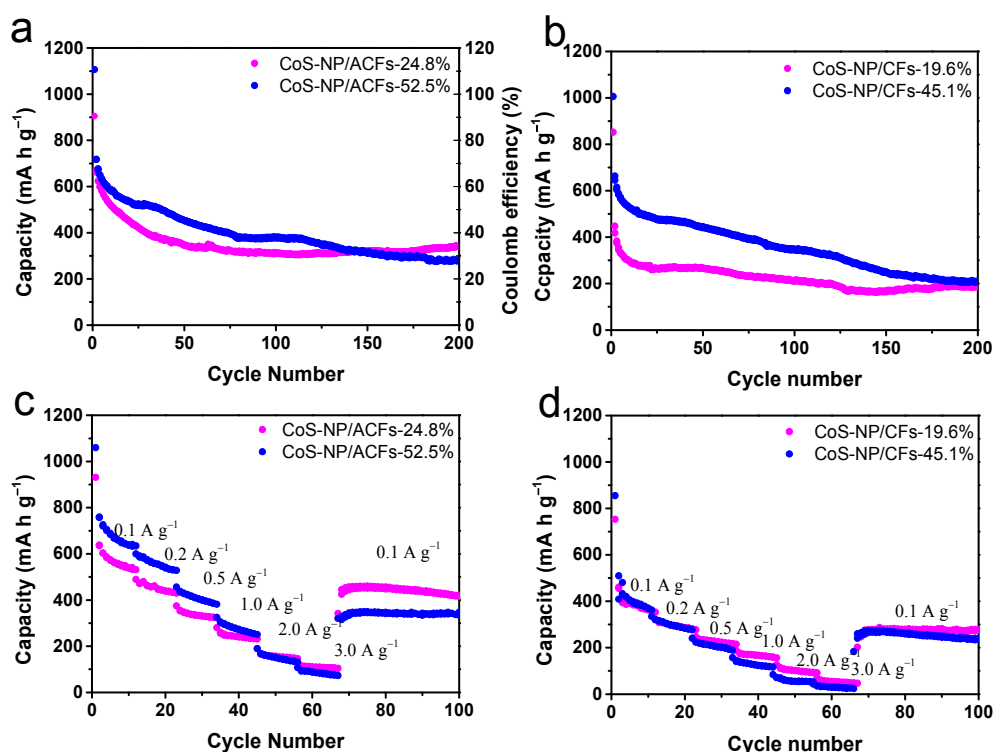


**Fig. S9** Electrochemical performance of the CoS-NP/ACFs and CoS-NP/CFs composites. The cycle performance of the CoS-NP/ACFs (a) and the CoS-NP/CFs (b) composites based anodes at a current density of 100 mA g<sup>-1</sup> between 0.01 and 3.0 V. The rate capabilities of the CoS-NP/ACFs (c) and the CoS-NP/CFs (d) composites based anodes at different current densities.

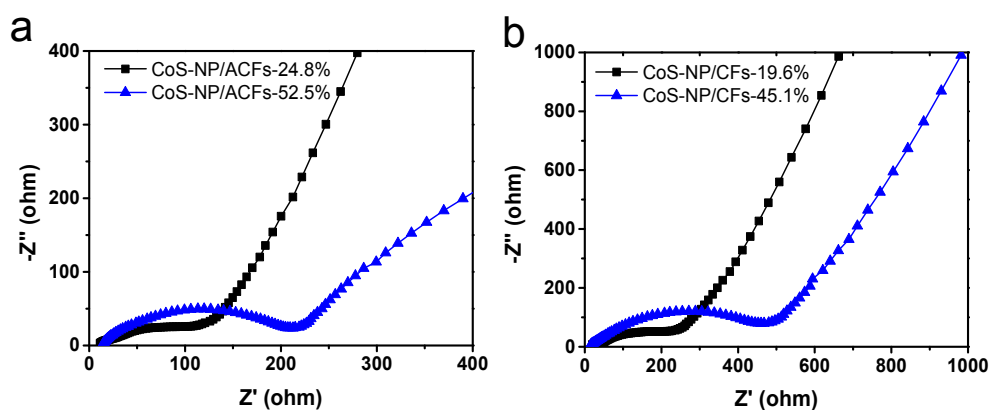


**Fig. S10** Nyquist plots of a) the CoS-NP/ACFs-24.8% and CoS-NP/ACFs-52.5% composites and b) the CoS-NP/CFs-19.6% and CoS-NP/CFs-45.1% composite after 20 charge/discharge cycles at the current density of 100 mA g<sup>-1</sup>.